

**Transient response of nonlinear magneto-optic rotation in a paraffin-coated Rb vapor cell**

M. Ummal Momeen and G. Rangarajan

*Department of Physics, Indian Institute of Technology, Chennai, Tamil Nadu 600 036, India*

Vasant Natarajan\*

*Department of Physics, Indian Institute of Science, Bangalore, Karnataka 560 012, India*

(Received 25 August 2009; published 25 January 2010)

We study resonant nonlinear magneto-optic rotation (NMOR) in a paraffin-coated Rb vapor cell as the magnetic field is swept. At low sweep rates, the nonlinear rotation appears as a narrow resonance signal with a linewidth of about “300  $\mu\text{G}$ ” ( $2\pi \times 420$  Hz). At high sweep rates, the signal shows transient response with an oscillatory decay. The decay time constant is of order 100 ms. The behavior is different for transitions starting from the lower or the upper hyperfine level of the ground state because of optical pumping effects.

DOI: [10.1103/PhysRevA.81.013413](https://doi.org/10.1103/PhysRevA.81.013413)

PACS number(s): 32.80.Qk, 42.50.Gy, 42.50.Hz, 42.50.Md

**I. INTRODUCTION**

It is well known that the plane of polarization of near-resonant light passing through an atomic vapor rotates in the presence of a magnetic field. In effect, the direction of the magnetic field breaks the symmetry of the system and thus induces birefringence. This magneto-optic rotation (MOR) also shows *nonlinear* effects when the light field is sufficiently strong, as can be produced by a laser. Such nonlinear magneto-optic rotation (NMOR) [1] arises because the response of the medium becomes light dependent. In other words, the light field, through optical pumping among the magnetic sublevels (causing alignment of the atom) or induced coherences between the sublevels, causes additional birefringence.

NMOR in atomic vapor has potential applications in sensitive magnetometry [2,3], search for a permanent electric dipole moment (EDM) [4], and magnetic resonance imaging (MRI) [1]. Because the ground-state coherence plays an important role in the phenomenon, the use of buffer-gas filled cells [5] or paraffin coating on the walls [6] is common in NMOR studies. For example, in Rb the vapor density is about  $10^9$  atoms/cm<sup>3</sup> at room temperature, which means that the mean free path is several orders of magnitude longer than the typical cell size. Thus, the ground-state coherence can be destroyed by spin-exchange collisions with the walls. It was shown that the use of paraffin coating on the walls [6] reduces the ground-state depolarization rate and enhances the optical pumping signals, with coherence lifetimes of order 1 s being observed.

In this work, we study the transient evolution of NMOR in a paraffin-coated Rb vapor cell, which gives important insight into the relaxation mechanisms. We observe evolution with a period of order 100 ms. The evolution depends on the laser power and the particular hyperfine transition being used, which in turn highlights the importance of optical pumping effects. The transient response can be understood qualitatively based on a density-matrix analysis of the system.

Systems exhibiting electromagnetically induced transparency (EIT) [7,8], electromagnetically induced absorption

(EIA) [9,10], and coherent population trapping (CPT) [11,12], were studied for their transient behavior. These studies show that the transient response occurs due to rapid switching on of the coupling field [13] or due to a sudden change of the Raman resonance condition [14,15]. Transient evolution is found to be of the order of microseconds in EIT and EIA systems, while it is of the order of tens of milliseconds in CPT systems, where again ground-state coherence plays an important role. The relatively long evolution time of the order of 100 ms seen in our studies of NMOR leads to potential applications in quantum information storage devices and nonlinear optical media with time-resolved gratings.

In nuclear magnetic resonance (NMR), adiabatic rapid passage conditions [16] lead to transient oscillations (called wiggles). This is because the magnetic field is swept across the resonance at a rate that is fast compared to the inverse relaxation times, as a consequence beats occur between the resonance signal and the signal induced by the precession of magnetization. The transient oscillations play an important role in calculating magnetic field inhomogeneities and the diffusion constant [17]. We observe similar transient oscillations in our studies here.

**II. THEORETICAL FORMALISM**

We used a density-matrix analysis of the system to understand the optical pumping and coherence effects that cause the nonlinear features of the magneto-optic rotation. The simplest model is to take a  $F = 1 \rightarrow F' = 0$  transition forming a three-level  $\Lambda$  system in the presence of a magnetic field, as shown in Fig. 1. The ground level splits into three sublevels, with energy shifts given by

$$\hbar \Delta_m = \mu_B g_F m_F B, \quad (1)$$

where  $\mu_B = 1.4$  MHz/G is the Bohr magneton,  $g_F$  is the Landé  $g$  factor,  $m_F$  is the magnetic quantum number, and  $B$  is the magnetic field. The upper level remains unsplit. Thus, the  $m_F = \pm 1$  ground sublevels form a three-level system with the  $m_{F'} = 0$  excited sublevel, coupled by opposite circular polarizations of light ( $\sigma^\pm$ ). Because of the opposite energy shifts for the  $m_F = \pm 1$  sublevels, the two circularly polarized components see opposite detunings, which is the origin of the magneto-optic rotation.

\*vasant@physics.iisc.ernet.in; www.physics.iisc.ernet.in/~vasant

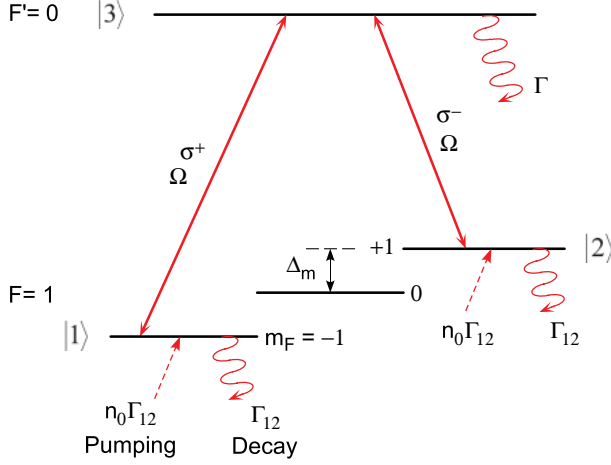


FIG. 1. (Color online) Three-level  $\Lambda$  scheme for a  $F = 1 \rightarrow F' = 0$  transition in the presence of a magnetic field.

The laser coupling the two levels is taken to have a Rabi frequency of  $\Omega$  (on resonance). The decay rate of the ground sublevels is  $\Gamma_{12}$ , while that of the upper level is  $\Gamma$ . Optical pumping into the ground sublevels is incorporated by taking a population pumping rate of  $n_0\Gamma_{12}$  into each sublevel. The susceptibilities for the two circularly polarized components are related to the density-matrix elements as

$$\begin{aligned}\chi^+ &= \frac{-2N\mu_{13}^2}{\hbar\epsilon_0\Omega} \tilde{\rho}_{13}, \\ \chi^- &= \frac{-2N\mu_{23}^2}{\hbar\epsilon_0\Omega} \tilde{\rho}_{23},\end{aligned}\quad (2)$$

where  $N$  is the atomic density. The rotation of the angle of polarization is related to the difference in *refractive indices* for the two circularly polarized components. In a dilute vapor, where the refractive index is close to 1, this can be approximated as [18]

$$\phi = \pi k_p l \text{Re}(\chi^+ - \chi^-), \quad (3)$$

where  $k_p$  is the probe wave vector and  $l$  is the total interaction length.

We studied the transient evolution of NMOR at a constant magnetic field of 100 mG. There are nine coupled density-matrix equations, which we solved numerically as a function of time. The spontaneous decay rates are taken to be  $\Gamma = 2\pi \times 6$  MHz and  $\Gamma_{12} = 2\pi \times 0.1$  MHz and the pumping rate into each ground level is taken to be  $n_0\Gamma_{12} = N\Gamma_{12}/2$ . The results for three Rabi frequencies are shown in Fig. 2. The evolution shows an oscillatory increase toward a steady-state value, with the frequency of oscillations increasing with the Rabi frequency.

In the experiments, the magnetic field is swept at different rates. It is difficult to simulate this situation since the field and therefore the energy shifts are changing with time. However, we will see later that transient oscillations occur at high sweep rates, similar to the oscillations seen in our simulation. The rotation rapidly builds up to a nonzero value and then saturates to the linear MOR value. At the Rabi frequency used in the experiment, the linear MOR value is close to zero so the

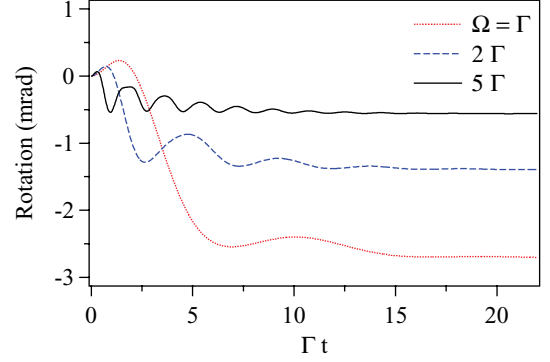


FIG. 2. (Color online) Calculated rotation for a  $F = 1 \rightarrow F' = 0$  transition as a function of time. The magnetic field is 100 mG.

rotation decays to zero. This behavior can be written in a qualitative manner as

$$\phi = A \exp(-Ct) \cos(\alpha t + \xi) - B \exp(-Dt) \cos(\beta t + \gamma), \quad (4)$$

where  $A, B, C, D, \alpha, \xi, \beta,$  and  $\gamma$  are constants that depend on the spontaneous decay rates, laser detuning, and the Zeeman shift. The total decay time constant is defined as

$$\tau = 1/C + 1/D. \quad (5)$$

### III. EXPERIMENTAL SETUP

The experimental schematic is shown in Fig. 3. The laser beams were derived from a home-built grating stabilized diode laser with a linewidth of 1 MHz [19]. It was locked to one of the hyperfine transitions of the  $D_2$  line of Rb using saturated-absorption spectroscopy in a vapor cell. The measurements were done in a 25-mm diameter  $\times$  50-mm long paraffin-coated vapor cell containing a natural mixture of Rb. The cell was kept inside a three-layer magnetic shield [20] that reduced the ambient fields to below 0.1 mG. The cell had an axial solenoid coil of dimensions 110-mm diameter by 360-mm length. The coil can produce fields up to 1 G, calibrated using a three-axis fluxgate magnetometer with 1 mG resolution. The field was

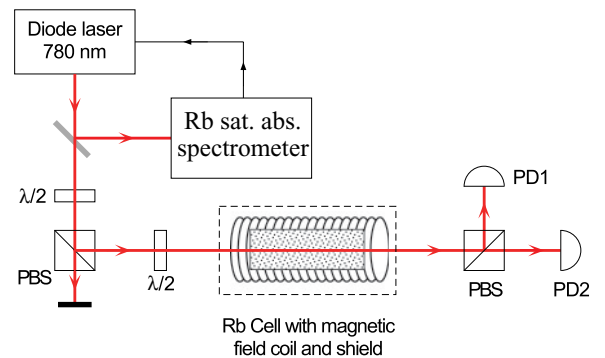


FIG. 3. (Color online) Schematic of the experiment. Figure labels:  $\lambda/2$ , halfwave retardation plate; polarizing beam splitter (PBS); photodiode (PD).

measured to be uniform to better than 1% over 100 mm (twice the cell length). The field was swept linearly using a function generator.

The laser beam in the experimental cell had a diameter of about 2 mm. The input was linearly polarized using a polarizing beamsplitter cube (PBS) and the output was split into its linear components again using a PBS. The two intensities,  $I_x$  and  $I_y$ , were made equal in the absence of a field (by adjusting the halfwave retardation plate in front of the cell). The rotation in the presence of a field was calculated from

$$\phi = \frac{1}{2} \arcsin \frac{I_x - I_y}{I_x + I_y}. \quad (6)$$

#### IV. RESULTS AND DISCUSSION

Resonant magneto-optic rotation in atomic vapor shows rapid variations even at magnetic fields of the order of mG. These rapid variations appear as resonances when the field is swept. Depending on the linewidth of the resonances they are classified as either *broad* or *narrow*. In general, linear MOR results in broad resonances and nonlinear MOR results in narrow resonances.

In this work we study the narrow NMOR resonances in Rb vapor. We measure NMOR in both isotopes of Rb,  $^{85}\text{Rb}$  and  $^{87}\text{Rb}$ , and in each isotope for transitions starting from either the lower or the upper ground hyperfine level. Since the relative transition strengths, the optical pumping rates, and the collision cross-sections change in the four cases, the different cases give us insight into the importance of these mechanisms.

##### A. NMOR for transitions from the lower hyperfine level

The first set of measurements was done for transitions starting from the lower hyperfine level. For the experiments in  $^{87}\text{Rb}$ , the laser was locked to the  $F = 1 \rightarrow F' = (1, 2)$  crossover resonance. The NMOR measurements were done at various magnetic field sweep rates and different laser powers. The laser power was relatively high, with a Rabi frequency of 1.5 to  $2\Gamma$ .

The narrow NMOR resonance seen when the field is swept at a slow rate of 0.8 mG/s is shown in Fig. 4(a). The high sensitivity ( $\sim 0.1$  mG) and narrow linewidth ( $300 \mu\text{G}$ ) of the resonance make it ideally suited for sensitive magnetometry at low field strengths. The sweep rate is quasistatic and therefore the rotation can be used to measure direct current DC fields. Of course, the actual application to magnetometry will require proper calibration of the field for a given light intensity and atomic density in the cell [2]. But it should be possible to use this effect to measure fields of order  $10 \mu\text{G}$ .

The resonance seen in Fig. 4(a) occurs due to two effects: (i) atoms that move away from the laser beam and have a coherent evolution longer than the transit time, and (ii) atoms returning into the interaction region of the beam after some spatial diffusion. Because the atoms spend most of the coherent evolution time outside the laser beam, the narrow resonances do not saturate with increasing laser power. By contrast, the broad resonances caused by linear MOR saturate at high laser power due to hole burning in the atomic velocity distribution.

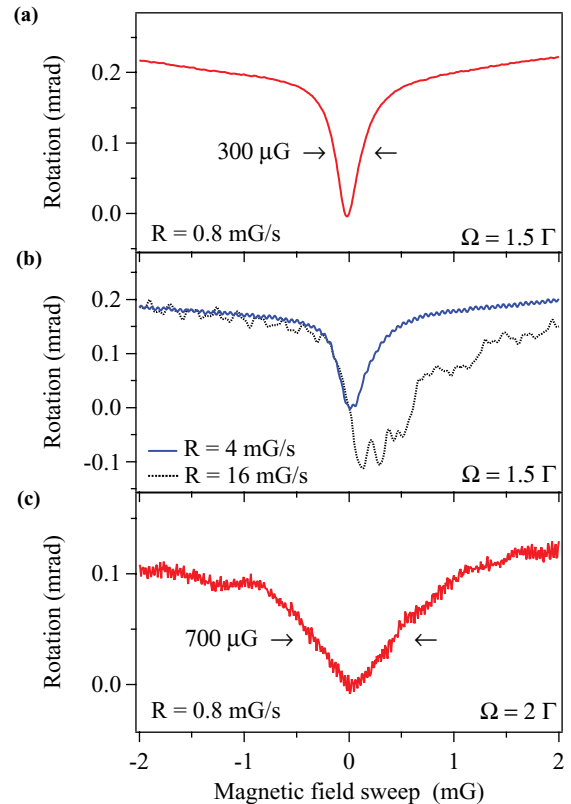


FIG. 4. (Color online) NMOR in the  $^{87}\text{Rb}$ ,  $F = 1 \rightarrow F' = (1, 2)$  transition. (a) Narrow resonance with a linewidth of  $300 \mu\text{G}$  with a magnetic sweep rate of 0.8 mG/s and  $\Omega = 1.5\Gamma$ . (b) Transient oscillations occur when the sweep rate is increased. (c) The linewidth increases as the Rabi frequency is increased to  $2\Gamma$ .

In our measurements, the laser power was high enough to saturate the broad resonance.

When the sweep rate is increased above 1 mG/s, the NMOR resonance structure begins to change. From the two curves shown in Fig. 4(b), it can be seen that the narrow resonance gradually disappears and transient oscillations begin to appear. The rotation decays after the resonance. The linewidth also increases when the laser intensity is increased to  $2\Gamma$ , as shown in Fig. 4(c).

When the magnetic field sweep rate is further increased to 160 mG/s, the rotation shows an oscillatory decay, as shown in Fig. 5. Note that the field reaches a value of 100 mG, compared to the 2 mG in Fig. 4. The rotation appears to follow the theoretical behavior predicted by Eq. (4). A curve fit of this equation to the measured rotation in Fig. 5(a) (measured at a Rabi frequency of  $1.5\Gamma$ ) fits the data well. All eight parameters in the equation are left as fit parameters. The best fit yields a time constant of 179.6 ms with a relative error of less than 1 part in  $10^5$ . The spin-exchange rate for  $^{87}\text{Rb}$  is 0.5508 Hz [21] and the Larmor precession frequency, defined as

$$\nu_0 = \frac{g_s \mu_B B}{(2I + 1)\hbar}, \quad (7)$$

has a value of 69.950 kHz at 100 mG. Thus, the spin-exchange rate is slower than the Larmor precession frequency, which shows that spin-exchange relaxation plays an important role. When the laser intensity is increased to  $2\Gamma$ , the decay constant

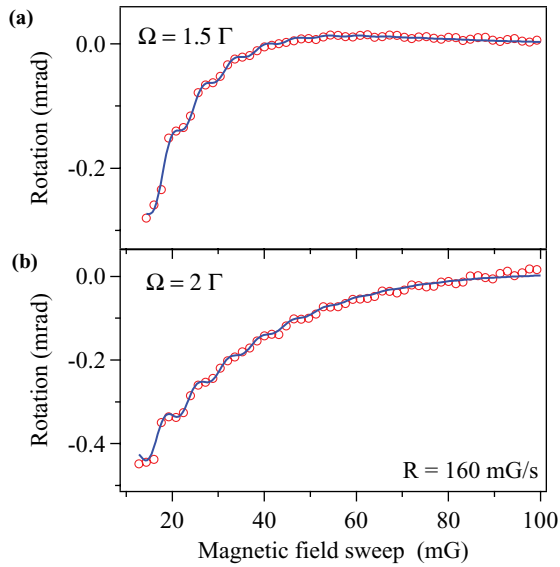


FIG. 5. (Color online) Transient evolution of NMOR in the  $^{87}\text{Rb}$ ,  $F = 1 \rightarrow F' = (1, 2)$  transition at a high sweep rate of 160 mG/s. (a) and (b) are for two values of the Rabi frequency. The open circles represent the measured rotation, while the solid lines are curve fits to Eq. (4).

[Fig. 5(b)] increases to 286.9 ms. This is consistent with the increase in linewidth with laser intensity seen in Fig. 4.

The behavior in the other isotope,  $^{85}\text{Rb}$ , is similar. The results with the laser locked to the  $F = 2 \rightarrow F' = (2, 3)$  transition at a power of  $1.5\Gamma$  are shown in Fig. 6. There is a narrow resonance peak with a linewidth of  $300 \mu\text{G}$  when the sweep rate is 0.8 mG/s. When the sweep rate is increased to 160 mG/s, the rotation shows a characteristic oscillatory

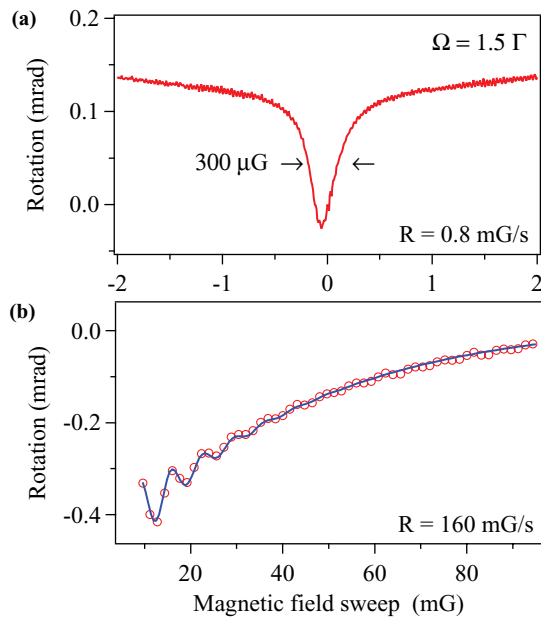


FIG. 6. (Color online) NMOR in the  $^{85}\text{Rb}$ ,  $F = 2 \rightarrow F' = (2, 3)$  transition. (a) Narrow resonance peak when the sweep rate is 0.8 mG/s. (b) Transient evolution (open circles) when the sweep rate is increased to 160 mG/s. The solid line is a curve fit to extract the decay time constant.

decay. Equation (4) describes the evolution quite well. A curve fit yields a time constant of 383.2 ms with a relative error of only  $3 \times 10^{-4}$ . The spin-exchange rate for  $^{85}\text{Rb}$  is 0.5866 Hz [21] and the Larmor precession frequency is 46.634 kHz at 100 mG. Thus, as in the case of  $^{87}\text{Rb}$ , the spin-exchange rate is slower than the Larmor precession frequency.

**B. NMOR for transitions from the upper hyperfine level**

Figure 7 shows the results of NMOR in  $^{85}\text{Rb}$  for transitions starting from the upper hyperfine level (i.e., with the laser locked to the  $F = 3 \rightarrow F' = 4$  transition). At low sweep rates, the rotation shown in Fig. 7(a) has a resonance peak, but the linewidth is  $850 \mu\text{G}$ , which is almost three times larger than the corresponding linewidth for the lower level transitions. The underlying reason for this increase is that the dominant transition for this set is the closed transition  $F \rightarrow F + 1$  (i.e.,  $3 \rightarrow 4$ ), while it is  $F \rightarrow F - 1$  for the lower level set. Since there are more magnetic sublevels in the upper state, optical pumping redistributes the population into one of the stretched magnetic sublevels.

The transient decay at high sweep rates, shown in Fig. 7(b), is similar to that for the lower level transition. Equation (4) models the decay reasonably well. A curve fit to this equation yields a decay time constant of 278 ms, but the relative error is quite large at 20%.

The behavior in  $^{87}\text{Rb}$  for upper level transitions (with the laser on the  $F = 2 \rightarrow F' = 3$  transition) shows a similar increase in linewidth at low sweep rates. But, in this particular case, the broad resonance does not saturate and the broad and narrow resonances coexist. This causes further broadening of the linewidth and nonsaturation of the rotation at high fields. The oscillations are also not seen clearly.

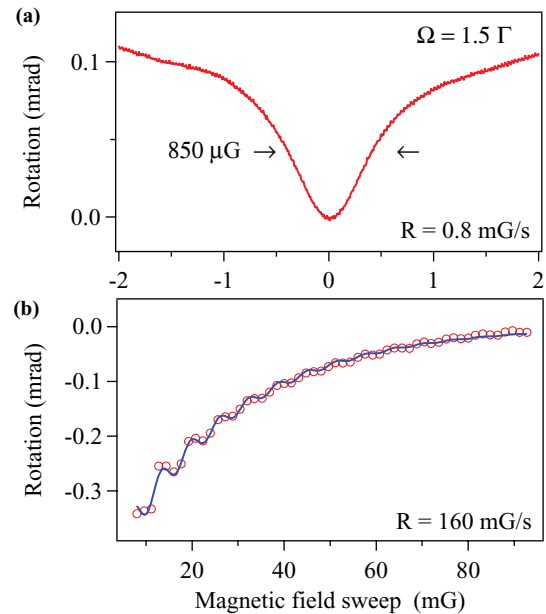


FIG. 7. (Color online) NMOR in the  $^{85}\text{Rb}$ ,  $F = 3 \rightarrow F' = 4$  transition. (a) Resonance peak when the sweep rate is 0.8 mG/s. (b) Transient evolution (open circles) when the sweep rate is increased to 160 mG/s. The solid line is a curve fit to extract the decay time constant.

## V. CONCLUSION

In conclusion, we studied nonlinear magneto-optic rotation in a paraffin-coated Rb vapor cell. The NMOR signal appears as a highly sensitive narrow resonance peak when the magnetic field is swept slowly. The linewidth is only  $300 \mu\text{G}$  for transitions starting from the lower ground hyperfine level, which can be useful for high sensitivity magnetometry. For upper-level transitions, the linewidth is much larger due to optical pumping among magnetic sublevels. When the field is swept at a high rate, the signal shows transient evolution with a characteristic oscillatory decay. The behavior can be understood qualitatively from a density matrix analysis of the system. The decay time constant depends on optical pumping rates, spontaneous decay rates, laser detuning, and the Zeeman

shift. The decay times are of order 100 ms, showing that spin-exchange collisions also affect the transient evolution. The long decay times appear to be a consequence of the increased coherence time in a paraffin-coated cell, though further experimental and theoretical studies are necessary to confirm this suggestion. Such long time constants can be useful in applications such as quantum information storage and time-resolved gratings.

## ACKNOWLEDGMENTS

This work was supported by the Department of Science and Technology, India. M.U.M. thanks IISc, Bangalore, for support and P. C. Deshmukh for guidance.

- 
- [1] D. Budker, W. Gawlik, D. F. Kimball, S. M. Rochester, V. V. Yashchuk, and A. Weis, *Rev. Mod. Phys.* **74**(4), 1153 (2002).
  - [2] D. Budker, D. F. Kimball, S. M. Rochester, V. V. Yashchuk, and M. Zolotarev, *Phys. Rev. A* **62**(4), 043403 (2000).
  - [3] M. Romalis and D. Budker, *Nat. Phys.* **3**(4), 227 (2007).
  - [4] D. F. Kimball, D. Budker, D. S. English, C.-H. Li, A.-T. Nguyen, S. M. Rochester, A. Sushkov, V. V. Yashchuk, and M. Zolotarev, in *Art and Symmetry in Experimental Physics*, edited by D. Budker *et al.* (AIP, New York, 2001), Vol. **596**, p. 84.
  - [5] I. Novikova, A. B. Matsko, and G. R. Welch, *J. Opt. Soc. Am. B* **22**(1), 44 (2005).
  - [6] M. A. Bouchiat and J. Brossel, *Phys. Rev.* **147**(1), 41 (1966).
  - [7] K.-J. Boller, A. Imamoglu, and S. E. Harris, *Phys. Rev. Lett.* **66**(20), 2593 (1991).
  - [8] S. E. Harris, *Phys. Today* **50**(7), 36 (1997).
  - [9] A. Lezama, S. Barreiro, and A. M. Akulshin, *Phys. Rev. A* **59**(6), 4732 (1999).
  - [10] C. Goren, A. D. Wilson-Gordon, M. Rosenbluh, and H. Friedmann, *Phys. Rev. A* **69**(6), 063802 (2004).
  - [11] E. Arimondo, *Progress in Optics* (Elsevier Science, Amsterdam, 1996), Vol. 35.
  - [12] R. Wynands and A. Nagel, *Appl. Phys. B* **68**, 1 (1999).
  - [13] P. Valente, H. Failache, and A. Lezama, *Phys. Rev. A* **65**(2), 023814 (2002).
  - [14] S. Gu and J. A. Behr, *Phys. Rev. A* **68**(1), 015804 (2003).
  - [15] S. J. Park, H. Cho, T. Y. Kwon, and H. S. Lee, *Phys. Rev. A* **69**(2), 023806 (2004).
  - [16] M. Garwood and L. DelaBarre, *J. Magn. Reson.* **153**(2), 155 (2001).
  - [17] G. D. Cates, D. J. White, T. R. Chien, S. R. Schaefer, and W. Happer, *Phys. Rev. A* **38**(10), 5092 (1988).
  - [18] A. K. Patnaik and G. S. Agrawal, *Opt. Commun.* **179**, 97 (2000).
  - [19] A. Banerjee, U. D. Rapol, A. Wasan, and V. Natarajan, *Appl. Phys. Lett.* **79**(14), 2139 (2001).
  - [20] Conetic AA Alloy, Magnetic Shield Division, Perfection Mica Co., Bensenville, Illinois, USA.
  - [21] H. W. Moos and R. H. Sands, *Phys. Rev.* **135**(3A), A591 (1964).